

Tuning the dynamic behavior of parametric resonance in a micromechanical oscillator

Wenhua Zhang,^{a)} Rajashree Baskaran, and Kimberly Turner

Department of Mechanical and Environmental Engineering, University of California at Santa Barbara, Santa Barbara, California 93106

(Received 3 September 2002; accepted 11 November 2002; publisher error corrected 13 January 2003)

We describe how to significantly change the dynamic behavior of parametric resonance in a micromechanical oscillator. By varying the voltage amplitude of applied electrical signal, the frequency response of the first order parametric resonance changes dramatically. We attribute this variation to the tuning of effective cubic stiffness of the oscillator, which is a contribution of both structural and electrical cubic stiffness. This phenomenon is well explained by the first-order perturbation analysis of nonlinear Mathieu equation. © 2003 American Institute of Physics. [DOI: 10.1063/1.1534615]

Resonant mode operation of micro- and nanoscale oscillators has found numerous applications in recent years with the advancement of fabrication and integration technologies. Electromechanical filters,¹ biological and chemical sensing,^{2,3} force sensing,^{4,5} and scanning probe microscopes⁶ are a few applications using resonant micro-oscillators. As technology allows for smaller scale features (hence decreasing amplitudes of motion), there are fewer reliable mechanical to electrical transduction mechanisms available. Thus, mechanical domain parametric amplification schemes^{7,8} are attractive. Parametric amplification schemes additionally have good noise rejection and broad bandwidths of operation.

In this letter, we demonstrate how, in a particular design of the electrostatic drive combs and mechanical spring, we can tune the effective cubic stiffness, thereby obtaining a wide range of qualitatively varying frequency responses. We focus on how tuning affects the parametric resonance characteristics of a sensor or oscillator. Parametrically driven oscillators show promise as filters, and with this technology a single oscillator can be tuned to function like a low-pass, high-pass, or bandpass filter. There is very good agreement with perturbation analysis of the model. This in turn offers tangible design guidelines to engineer the response characteristics, such as bandwidth and shape of the response, in terms of the design and operating parameters.

We have presented a study of parametric resonance in a micro electro mechanical (MEM) oscillator with cubic mechanical and electrostatic force terms elsewhere.⁹ A 2:1 sub-harmonic resonance (first-order parametric resonance) near the first resonance mode can be generated in an electrostatically actuated oscillator with time-varying effective stiffness. The dynamic response of the oscillator can be understood to a good degree when modeled with a nonlinear Mathieu equation.^{9,10} We have shown that the effective cubic nonlinearity, along with contributions from the mechanical constraints and electrostatic fringing field, plays an important role in the dynamic response of the oscillator.

The oscillator under study is fabricated by S. G. Adams¹¹

using SCREAM,¹² a bulk micro-machining technique for the independent tuning of linear and cubic stiffness terms (Fig. 1). The area of the device is about $500 \times 400 \mu\text{m}^2$. It has two sets of parallel interdigitated comb finger banks on either end of the backbone and two sets of noninterdigitated comb fingers on each side. The four crab-leg beams provide an elastic restoring force for the oscillator. The springs, backbone, and the fingers are $\sim 2 \mu\text{m}$ wide and $\sim 12 \mu\text{m}$ deep. Either the interdigitated or the noninterdigitated comb fingers may be used to drive the oscillator.

The experiments are performed in a multidimensional MEMS motion characterization suite.¹³ The oscillator is placed in a vacuum chamber with an ambient pressure of ~ 7 mTorr. The in-plane motion is detected by a laser doppler vibrometer (Polytec OFV-501/3001) through a 45° mirror. Velocity and displacement signals are recorded and analyzed through a spectrum analyzer (HP89470A) and an oscilloscope (TDS 420 A).

To actuate parametric resonance, a voltage signal is applied on the noninterdigitated comb fingers. A square root signal is used to avoid coupling with harmonic resonance.¹⁴

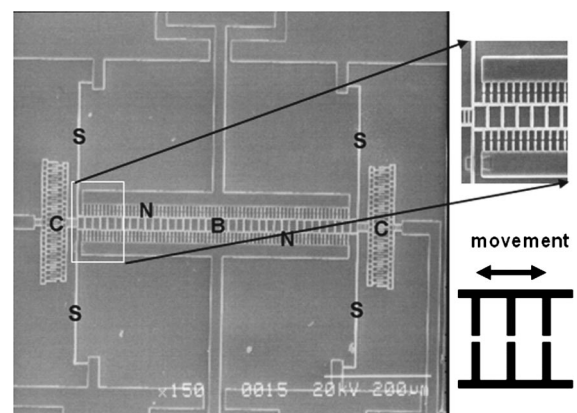


FIG. 1. A scanning electron micrograph of the oscillator. Note the folded beam springs (S), the two sets of interdigitated comb finger banks (C) on both ends of backbone (B) and noninterdigitated comb fingers (N) on each side of backbone (B). The noninterdigitated combfingers are such that they cause an effective linear electrostatic stiffness augmenting the mechanical stiffness.

^{a)}Electronic mail: whzh@enr.ucsb.edu

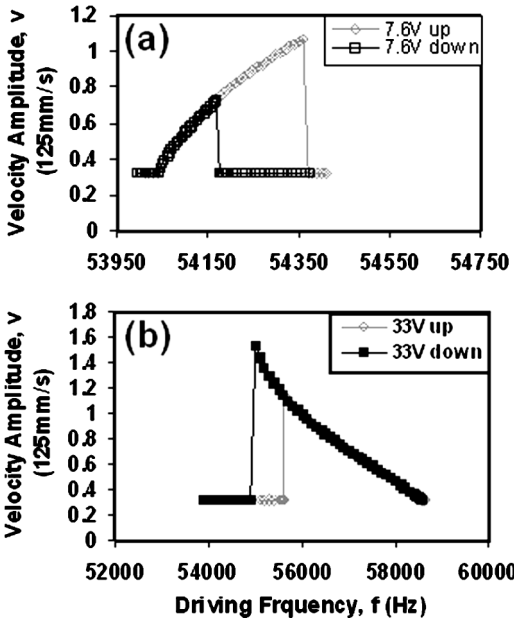


FIG. 2. The frequency response curve of parametric resonance at (a) $V_A = 7.6$ V and (b) $V_A = 33$ V. At $V_A = 7.6$ V, velocity signal increases as sweeping driving frequency up and a bistable state exists at the right side of resonance region. At $V_A = 33$ V, the velocity signal decreases as sweeping up driving frequencies and a bistable state exists at the left boundary.

At 7.6 and 33 V, the frequency responses of parametric resonance are shown in Figs. 2(a) and 2(b), respectively. Frequency is swept up (increasing) and down (decreasing) to capture the bistable state characteristics of parametric resonance.

At 7.6 V, when sweeping frequency up, the velocity signal increases and jumps from 1.07 down to 0.322 V at 54 380 Hz. When sweeping frequency down, the velocity signal jumps up to 0.716 V at 54170 Hz. In these two cases, the velocity response signals are the same at $f < 54170$ Hz, and are different at $f > 54170$ Hz. Bistable state exists at the right side of the resonance region, as shown in Fig. 2(a).

Opposite to $V = 7.6$ V, when sweeping frequency up at 33 V, the velocity signal jumps up from 0.324 to 1.142 V at 55630 Hz and decreases as frequency increases. When sweeping frequency down, the velocity signal increases and jumps down from 1.54 V to 0.32 at 55 000 Hz. The bistable state switches to the left boundary ($f = 55 630$ Hz) of the resonance region [see Fig. 2(b)].

We attribute this bifurcation switch to the effects of nonlinearity. In the oscillator shown in Fig. 1, when electrical signal is applied on the noninterdigitated comb fingers, the electrostatic force generated is dependent on the position of the oscillator. In the experiments presented here, we use a square root of the ac voltage signal [$V_A(1 + \cos 2\omega t)^{1/2}$] to isolate the parametric resonance from direct harmonic response.¹⁴ The movement of the device is governed by nonlinear Mathieu equation:⁹

$$\frac{d^2x}{d\tau^2} + \alpha \frac{dx}{d\tau} + (\beta + 2\delta \cos 2\tau)x + (\delta_3 + \delta'_3 \cos 2\tau)x^3 = 0, \tag{1}$$

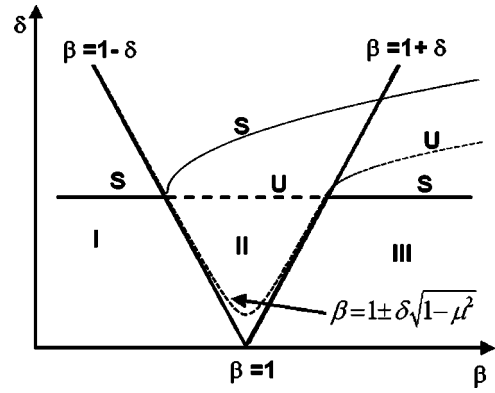


FIG. 3. Schematic of the characteristics of the first order parametric resonance. This figure is repeated from earlier work⁹ for clarity of discussion. $\beta = 1 \pm \delta\sqrt{1 - \mu^2}$ is the damping effect on the boundary of resonance region. S represents stable solution, while U represents unstable solution. The figure also shows how the stable (dark trace) and unstable (broken trace) solutions vary as β changes quasistatically with a constant δ .

where

$$\alpha = \frac{2c}{m\omega}, \quad \beta = \frac{4(k_1 + r_1 V_A^2)}{m\omega^2},$$

$$\delta = \frac{2r_1 V_A^2}{m\omega^2}, \quad \delta_3 = \frac{4k_3 + 4r_3 V_A^2}{m\omega^2}, \quad \delta'_3 = \frac{4r_3 V_A^2}{m\omega^2},$$

and m , k_1 , and k_3 are the mass, linear, and cubic mechanical stiffness of the oscillator, respectively, c is the damping coefficient, r_1 and r_3 are linear and cubic “electrostatic stiffness,” respectively, and $\tau = \omega t$ is a normalized time.

We use a two-variable expansion perturbation method¹⁵ to analyze Eq. (1). The detailed analysis is presented elsewhere;⁹ only the relevant results are discussed here. When the driving frequency is about two times the first resonant mode frequency of the oscillator and the drive amplitude is above a critical value, 2:1 subharmonics are generated. Assuming $\beta = 1 + \beta_1 \delta$, the amplitude and phase of this response within this range of frequencies is given by

$$R^{*2} = -\frac{4}{3\gamma_{3\text{eff}}} [\beta_1 + \cos(2\theta^*)], \tag{2}$$

$$\theta^* = 0, \frac{\pi}{2}, \pi, \frac{3\pi}{2}, \tag{3}$$

where $\gamma_{3\text{eff}}$ is the effective nonlinearity parameter (ENP) of the system, a sum of contributions from cubic mechanical stiffness, which is fixed for a particular beam design and voltage-dependent cubic electrostatic stiffness.

$$\gamma_{3\text{eff}} = \frac{1}{r_1 V_A^2} \left(2k_3 + \frac{10}{3} r_3 V_A^2 \right). \tag{4}$$

This result is schematically represented in Fig. 3. The solution characteristics of Eq. (2) depend on the sign of ENP. Let us assume the ENP is negative. In this case of $\theta^* = 0$ and π , $R^{*2} = -4(\beta_1 + 1)/(3\gamma_{3\text{eff}})$. A nontrivial stable solution exists at $\beta_1 > -1$ and a trivial solution is unstable. When $\theta^* = \pi/2$ and $3\pi/2$, $R^{*2} = -4(\beta_1 - 1)/(3\gamma_{3\text{eff}})$. At $\beta_1 > 1$, another nontrivial (unstable) solution exists and the trivial solution becomes stable. When ENP is positive, the schematic responses will be mirrored about a vertical axis at $\beta = 1$ and

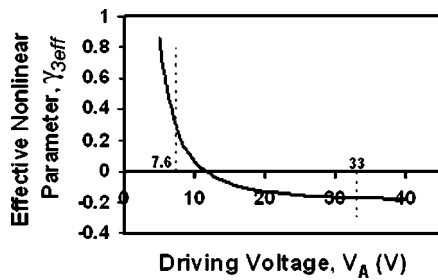


FIG. 4. The ENP as a function of the driving voltage amplitude V_A . Note the change of the sign of ENP corresponding to $V_A=7.6$ and $V_A=33$ V.

stability states of regions I and III are swapped. The growth of R^* with respect to β in different areas is also schematically shown in Fig. 3, where the solid line represents stable solution and dashed line represents unstable solution. Since $\beta_1 = \pm 1$ corresponds to transition curves from stable to unstable areas in β - δ plane, bifurcation occurs when we quasistatically vary frequency of the input voltage across the transition curve.

For the oscillator in our study, simulation results using boundary element method (electrostatic force calculation) and finite element method (mechanical stiffness calculation) show that the values of electrostatic stiffness parameters r_1 and r_3 are $3.3e-3 \mu\text{NV}^{-2} \mu\text{m}^{-1}$ and $-0.98e-3 \mu\text{NV}^{-2} \mu\text{m}^{-3}$ and mechanical cubic stiffness k_3 is $0.0437 \mu\text{N} \mu\text{m}^{-3}$. Figure 4 shows how ENP changes at different voltage amplitude of applies electrical signal. By varying the applied voltage, the value of ENP can be tuned and even switched from positive to negative. Note that the input voltage magnitude at which this shift in the ENP sign occurs at ~ 12 V, which is very small compared to the isolation layer breakdown voltage for the bulk micromachined device. While we studied a similar device previously,⁹ the magnitude and signs of the linear and cubic electrostatic stiffness made it impossible to observe this shift in the sign of ENP.

Figures 2(a) and 2(b) experimentally show such changes as we vary the applied voltage. As schematically shown in Fig. 4, at lower voltage (7.6 V), ENP is positive. A corresponding bistable state exists at the right boundary. When the applied voltage is increased to higher voltage (33 V), ENP becomes negative and the bistable state switches to the left boundary.

In conclusion, we have demonstrated that tuning the effective nonlinear stiffness can drastically change the frequency response of an autoparametric oscillator. The effective nonlinear parameter of the oscillator is a critical parameter in such changes. A perturbation analysis of the governing nonlinear Mathieu equation sheds light on the effect of cubic nonlinearity on frequency response. Experimental results agree well with the analysis. It is been demonstrated that the ENP of the oscillator can be tuned to have frequency responses which can be utilized as a low-pass, high-pass or bandpass filter within the region of parametric resonance excitation.

- ¹C. T. C. Nguyen, *Smart Structures and Materials 1999: Smart Electronics and MEMS, Newport Beach, California, 1-3 March 1999* (SPIE, Bellingham, WA, 1999), p. 55.
- ²B. Ilic, D. Czaplewski, H. G. Craighead, P. Neuzil, C. Campagnolo, and C. Batt, *Appl. Phys. Lett.* **77**, 450 (2000).
- ³M. K. Baller, H. P. Lang, J. Fritz, C. Gerber, J. K. Gimzewski, U. Drechsler, H. Rothuizen, M. Despont, P. Vettiger, F. M. Battiston, J. P. Ramseier, P. Fornaro, E. Meyer, and H. J. Guntherodt, *International Conference on Scanning Probe Microscopy, Cantilever Sensors and Nanostructures, Seattle, Washington, 30 May-1 June 1999* (Elsevier, Netherlands, 2000), p. 1.
- ⁴T. D. Stowe, K. Yasumura, T. W. Kenny, D. Botkin, K. Wago, and D. Rugar, *Appl. Phys. Lett.* **71**, 288 (1997).
- ⁵T. Kenny, *IEEE Sens. J.* **1**, 148 (2001).
- ⁶D. Rugar, C. S. Yannoni, and J. A. Sidles, *Nature (London)* **360**, 563 (1992).
- ⁷K. L. Turner, S. A. Miller, P. G. Hartwell, N. C. Macdonald, S. H. Strogartz, and S. G. Adams, *Nature (London)* **396**, 149 (1998).
- ⁸A. Olkhovets, D. W. Carr, J. M. Parpia, and H. G. Craighead, *Technical Digest, MEMS 2001, 14th IEEE International Conference on Micro Electro Mechanical Systems, Interlaken, Switzerland, 21-25 Jan. 2001* (IEEE, Piscataway, NJ, 2001), p. 298.
- ⁹W. Zhang, R. Baskaran and K. L. Turner, *Sens. Actuators A* **102**, 139 (2002).
- ¹⁰R. Grimshaw, *Nonlinear Ordinary Differential Equations* (CRC, Boca Raton, FL, 1993).
- ¹¹S. G. Adams, F. M. Bertsch, K. A. Shaw, and N. C. Macdonald, *J. Microelectromech. Syst.* **7**, 172 (1998).
- ¹²N. C. Macdonald, *Microelectron. Eng.* **32**, 49 (1996).
- ¹³K. L. Turner, *Digest of Technical Papers, Transducers'99, The 10th International Conference on Solid-State Sensors and Actuators, Sendai, Japan, 7-10 June 1999* (unpublished).
- ¹⁴K. L. Turner, P. G. Hartwell, F. M. Bertsch, and N. C. Macdonald, *ASME International Mechanical Engineering Congress and Exposition Proceedings of Microelectromechanical Systems (MEMS), Anaheim, CA, 15-20 Nov. 1998* (ASME, New York, 1998), p. 335.
- ¹⁵R. H. Rand, *Lecture Notes on Nonlinear Vibrations, Version 34a* [available at <http://www.tam.cornell.edu/randdocs>], 2000.